

CrossMark
click for updatesCite this: *Catal. Sci. Technol.*, 2016,
6, 5320Received 25th March 2016,
Accepted 21st April 2016

DOI: 10.1039/c6cy00654j

www.rsc.org/catalysis

The importance of heat effects in the methanol to hydrocarbons reaction over ZSM-5: on the role of mesoporosity on catalyst performance†

Irina Yarulina, Freek Kapteijn and Jorge Gascon*

Interpretation of catalytic performance during the MTH process is hampered by heat transport phenomena. We demonstrate that large temperature rises can occur during fixed bed lab-scale catalyst testing of ZSM-5, even when a large catalyst bed dilution is applied. Formation of mesopores in ZSM-5 leads to partial mitigation of these effects because of a lower generation of heat per unit catalyst volume and weakening of the zeolite acidity.

1. Introduction

The methanol-to-hydrocarbons (MTH) process comprises the conversion of methanol over acidic zeolites. Although this process was patented already in 1977¹ and widely applied since 2010 at the industrial level,² there is currently a great interest in improving selectivity towards propylene and in enhancing catalyst lifetime. In order to achieve this objective, many scientific publications focus on the application of mesoporous zeolites to prolong catalyst lifetime *via* improving diffusion properties.^{3–6} Despite the initial success of mesoporous zeolites in MTH catalysis,^{7,8} some recent studies have shown that not every mesoporous zeolite is equally effective.^{9,10} In this line, Michels *et al.*¹¹ have shown that, under industrially relevant conditions, blends of microporous zeolites and binders can easily outperform purely mesoporous catalysts.

In contrast to the huge efforts devoted to materials development, very little effort has been devoted to studies at the reactor level, something surprising considering the high exothermicity of the reaction (the reaction enthalpy of methanol dehydration is -24 kJ mol^{-1} , while reaction enthalpies of the olefins formation vary from -11 kJ mol^{-1} for ethylene to -53 kJ mol^{-1} for butene).¹² Guo *et al.*¹³ calculated for a single-bed adiabatic reactor an adiabatic temperature rise of more than 200 °C, which will obviously result in accelerated coke deposition, possible catalyst degradation and a different product scope under these highly nonisothermal conditions. In turn, analysis of literature reveals controversial results^{8,11} reported for the same catalytic system (ZSM-5, Zeolyst, Si/Al = 40) and/or

catalysts with similar physicochemical properties¹⁴ tested under alike conditions. These results suggest that reactor configuration together with heat and mass transport are of high importance when it comes to catalyst lifetime and process selectivity. Here, we highlight the large impact of catalyst testing conditions on data reproducibility and catalyst deactivation.¹⁵ Taking mesoporous zeolites as case study, we demonstrate that active site isolation and its consequences for catalyst acidity and heat generation are the main reasons behind improved lifetime and selectivity, rather than the usually claimed improvement of diffusion properties.

2. Experimental

2.1. Catalyst preparation

ZSM-5 zeolite (Si/Al = 40) was purchased from Zeolyst. Mesoporous ZSM-5 was prepared by desilication with 1 M NaOH at 70 °C for 1 h followed by acid leaching in 1 M HNO₃ aqueous solution to remove extraframework Al. The post synthetic method for the production of mesoporous ZSM-5 was adapted from Sartipi *et al.*¹⁶ as follows. ZSM-5 in the ammonium form was calcined at 550 °C for 5 h to obtain the parent H-ZSM-5. Desilication of H-ZSM-5 powder was carried out in 1 M NaOH aqueous solution in a capped vessel ($\text{volume}_{\text{basesolution}}/\text{mass}_{\text{parentH-ZSM-5}} = 8.0 \text{ cm}^3 \text{ g}^{-1}$) and under stirring at 70 °C for 1 h in an oil bath. This treatment was followed by immediate quenching in a water-ice bath and centrifugation to separate the zeolite powder from the solution. The residue of the desilicating agent was removed from the zeolite crystallites by subsequent redispersion in deionized water and centrifugation cycles until neutral pH was reached. Desilicated ZSM-5 was dried overnight at 120 °C for 12 h and calcined at 550 °C for 5 h. Yield of the desilication procedure was 25% (averaged from four experiments starting from *ca.* 20 g of H-ZSM-5).

Catalysis Engineering, Chemical Engineering Department, Delft University of Technology, Julianalaan 136, 2628 BL Delft, The Netherlands.
E-mail: J.Gascon@tudelft.nl

† Electronic supplementary information (ESI) available. See DOI: 10.1039/c6cy00654j



Subsequently, desilicated ZSM-5 was acid treated in 1 M HNO_3 aqueous solution (volume_{acid solution}/mass_{zeolite} = 28.6 $\text{cm}^3 \text{g}^{-1}$) at 70 °C 2 h under stirring in an oil bath. After quenching, the sample was thoroughly washed with deionized water, dried and calcined the same as after the above mentioned desilication procedure.

2.2. Catalyst characterization

N_2 adsorption at 77 K was carried out using the Tristar II 3020 analyzer (Micromeritics). Prior to the experiment, samples were outgassed at 350 °C for 16 h.

Scanning microscopy (SEM) images were recorded using a JEOL JSM-6010LA with a standard beam potential of 10 kV and an Everhart-Thornley detector. X-ray microanalysis (SEM/EDX) confirmed the elemental composition in the sample by (SEM) coupled to a dispersive X-ray microanalysis system (EDX) with a silicon-drift detector.

The XRD patterns of the powders were recorded in Bragg-Brentano geometry with a Bruker D8 Advance X-ray diffractometer equipped with a LynxEye position-sensitive detector. Measurements were performed at RT by using monochromatic $\text{CoK}\alpha$ ($\lambda = 1.788970 \text{ \AA}$) radiation between $2\theta = 5^\circ$ and 50° .

Temperature-programmed NH_3 desorption (NH_3 -TPD) was measured by an AutoChem II chemisorption analyzer (Micromeritics). Approximately 0.2 g of the material was first degassed under He flow at 400 °C and then saturated with NH_3 at 200 °C during 1 h using a flow of 1.65% NH_3 in He. The gas mixture was then switched back to He and the sample was purged at 200 °C for about 1 h to remove weakly adsorbed NH_3 molecules. TPD was subsequently recorded under He flow, from 200 °C to 800 °C. All flow rates were adjusted to 25 mL min^{-1} , and the heating rates were 10 °C min^{-1} during different stages of experiment.

Transmission FT-IR spectroscopy using pyridine as a probe molecule was performed using a Nicolet 6700 spectrometer equipped with MCT/B detector. The zeolite samples were activated in vacuum at 400 °C for 16 h to remove adsorbed species. After activation, pellets were saturated with pyridine vapor and further evacuated at 160 °C for 2 h. Spectra were recorded in 1000–4000 cm^{-1} range at 4 cm^{-1} resolution and co-addition of 128 scans. The amount of Brønsted (BAS) and Lewis (LAS) acid sites was derived from the bands at 1545 and 1456 cm^{-1} as described elsewhere.¹⁷

2.3. Catalyst testing

Catalytic experiments were carried out in a Microactivity Reference unit (PID Eng&Tech) at 400–500 °C and ambient pressure as described elsewhere.¹⁸ The catalyst (pressed, crushed and sieved to particle sizes 250–420 μm) was placed in a fixed-bed reactor with internal diameter 9 mm equipped with three thermocouples monitoring the temperatures at different heights inside the catalytic bed during MTH experiments and catalyst regeneration. Another thermocouple in contact with the reactor wall was used to control temperature. Reaction lifetime was investigated as a function of temperature,

degree of catalyst dilution with SiC ($m_{\text{cat}}:m_{\text{SiC}} = 1:0\text{--}6$) and reactor diameter (4, 7, 9 mm).

Catalyst regeneration was achieved by a continuous flow of a mixture of N_2 (30 mL min^{-1}) and air (30 mL min^{-1}) for 8 h at 550 °C followed by cooling down the catalytic bed to reaction temperature under N_2 flow (30 mL min^{-1}).

An HPLC pump (307 5-SC-type piston pump, Gilson) was used to feed methanol to the reactor system. Weight-hourly space velocities (WHSV) of 8 and 4 $\text{g}_{\text{MeOH}} \text{g}_{\text{cat}}^{-1} \text{h}^{-1}$, a 1:1 molar feed composition of N_2 and MeOH and atmospheric pressure were utilized.

Conversion, selectivities and yields were calculated on a molar carbon basis. Detailed information on calculations together with dilution experiments can be found in ESI†

The performance results are presented in graphs as a function of the methanol throughput per amount of catalyst used ($\text{g}_{\text{MeOH}} \text{g}_{\text{cat}}^{-1}$) and defined as overall MeOH throughput fed through the catalytic bed before the conversion of oxygenates drops below 90%.

3. Results and discussion

First of all, catalyst deactivation was studied as a function of reaction temperature, always using undiluted fresh ZSM-5. In line with the literature available,^{11,19,20} the catalyst lifetime depends on reaction temperature: it decreases from 27 to 10 h when temperature rises from 400 °C to 500 °C (Fig. 1a). Moreover, selectivity to C2–C4 olefins increases from 28 to 52%, indicating a much higher selectivity to propylene at higher temperatures (Fig. 1b).

Considering the relatively high partial pressure of methanol in the feed (0.5 bar) and operation at full conversion, conditions commonly used in the MTH reaction, utilization of a catalyst bed diluent such as silicon carbide (SiC) is of high importance, mainly because of the improved heat conduction in the bed, the lower heat production per unit volume, the larger wall heat exchange area, and a decreased effect of axial dispersion.^{21,22} Indeed, dilution of catalyst with an inert is frequently, but not always, applied in MTH catalytic tests at the laboratory scale.^{11,23,24}

Therefore, in addition to the above mentioned experiments, the same parent ZSM-5 catalyst was tested in the presence of different amounts of SiC (ZSM-5:SiC = 1:3 and 1:6 wt/wt, equivalent to 1:0.9 and 1:1.8 vol/vol, see ESI†). These

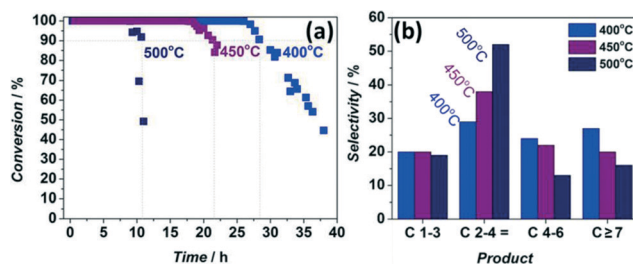


Fig. 1 Conversion versus time-on-stream (a) and corresponding integral product selectivities (b) for different temperatures over ZSM-5. WHSV = 8 h^{-1} , $\text{MeOH}:\text{N}_2 = 1:1$, reactor ID 9 mm.



experiments clearly demonstrate the strong effects of heat generation on catalyst deactivation (Fig. 2). At 400 °C, catalyst lifetime increased from 27 to 52 h, independent of the chosen ZSM-5 to SiC ratio (Fig. 2a). At 450 °C, there is a slight lifetime difference of 3 h depending on the chosen ratio (Fig. 2b). Thus, by choosing appropriate amount of diluent (catalyst:SiC = 1:6 wt/wt or 1:1.8 vol/vol) the catalyst lifetime could be extended by a factor of two at all studied temperatures. These data already indicate the strong non-isothermal behaviour of the process and the necessity to take measures to ensure isothermal operation, such as using an appreciable amount of diluent. On the other hand, a too large degree of dilution may lead to an inhomogeneous catalyst distribution and feed bypassing, meaning that an optimum has to be found in every case.²²

To follow heat dispersion in the axial direction, the same experiments were performed while monitoring the tempera-

ture at different positions inside the catalytic bed as a function of time. The data obtained for pure ZSM-5 (no dilution) under conditions generally applied in literature demonstrate a temperature rise inside the reactor of 80 °C (Fig. 3a₁). Moreover the three temperature maxima confirm a moving active zone behaviour during MTH reaction.^{25–28} Once the first region of the bed has deactivated, which corresponds to the first temperature maximum of 547 °C, observed after 12 h TOS, the reaction zone slowly moves downwards. The third maximum coincides with MeOH breakthrough, indicating full catalyst deactivation. The observed difference in maximum temperature rise between the first and second thermocouple (around 20 °C) and the fact that the product composition at the exit of the reactor is not constant (Fig. 3a₂) are also in line with the moving reaction zone behaviour during MTH. In such a scenario, primary products of MTH at the top of the bed would further interact with the fresh zeolite downstream, partly deactivating the catalyst and resulting in less heat released in the lower part of the reactor. Differences in product distribution *versus* time-on-stream could also be explained on the same grounds. Furthermore, considering the large temperature increase and the fact that water is the main product of MTH, stability of the zeolite framework under the applied conditions (*in situ* steaming) may be a special point of concern that would also explain the highlighted literature inconsistencies.^{29–31}

To verify the latter hypothesis, the deactivated catalyst was subjected to two additional runs under the same reaction conditions with oxidative regeneration steps in between. Fig. 4 and 5 show that the catalyst lifetime had increased by

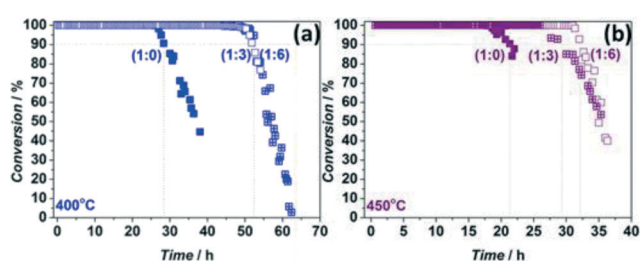


Fig. 2 Conversion as a function of time-on-stream over ZSM-5 diluted with different amounts of SiC at 400 °C (a) and at 450 °C (b). ZSM-5:SiC = 1:0; 1:3; 1:6 wt/wt. WHSV = 8 h⁻¹, MeOH:N₂ = 1:1, reactor ID 9 mm.

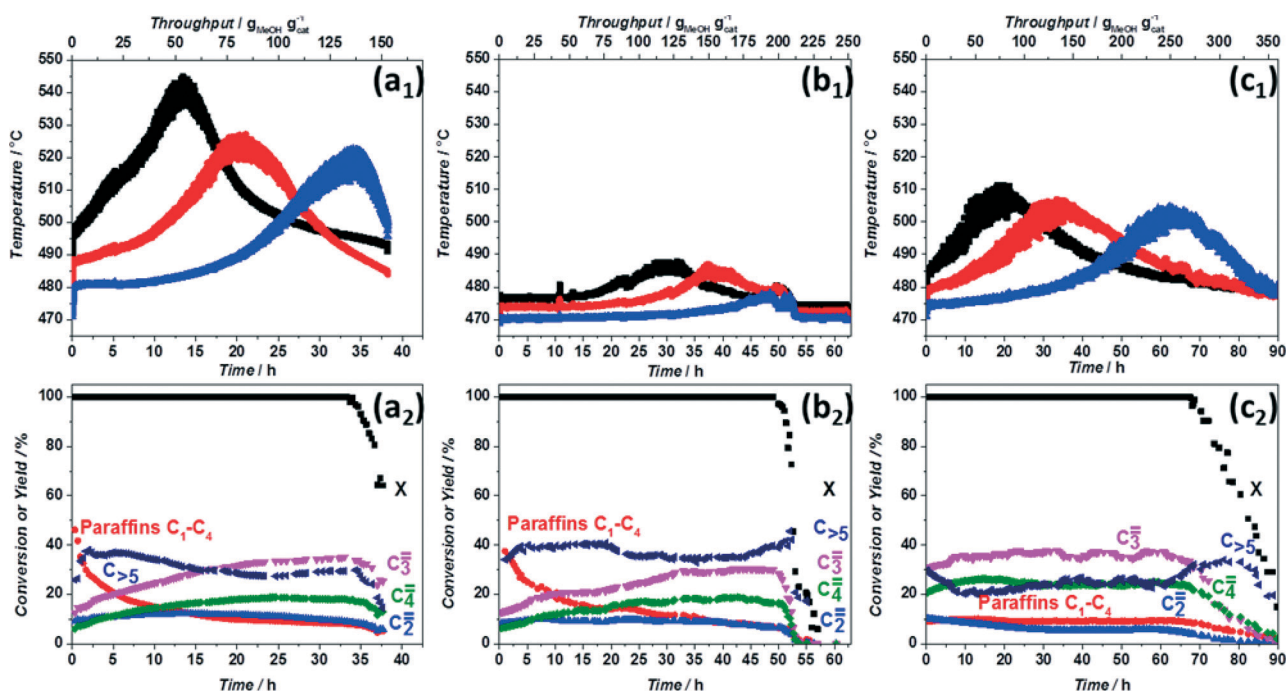


Fig. 3 Temperature profiles (a₁, b₁, c₁) and corresponding product distribution (a₂, b₂, c₂) as a function of time-on-stream for ZSM-5 (a₁, a₂), ZSM-5:SiC = 1:6 wt/wt (b₁, b₂) and mesoporous ZSM-5 (c₁, c₂). Set-point temperature 470 °C, L_{bed} = 5 cm, WHSV = 4 h⁻¹, MeOH:N₂ = 1:1. C_{>5} indicates hydrocarbons with 5 or more C atoms.



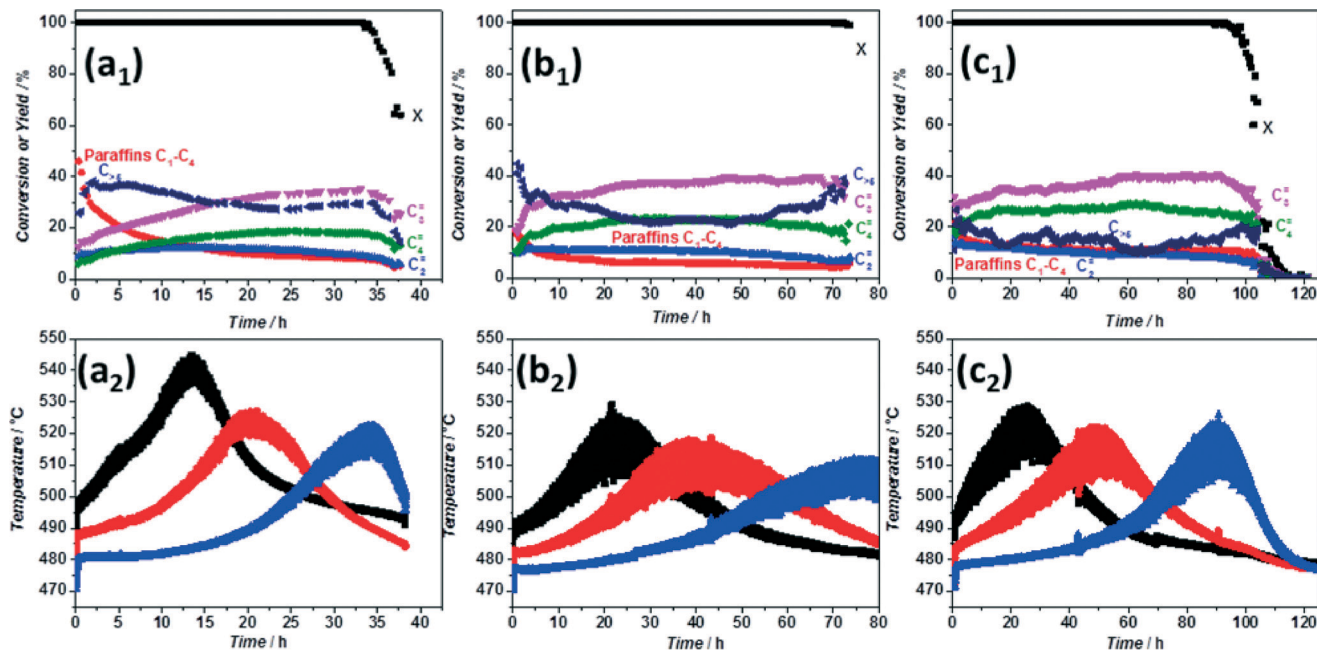


Fig. 4 Temperature profiles (a₂, b₂, c₂) and corresponding product distribution (a₁, b₁, c₁) as a function of time-on-stream for undiluted ZSM-5 during three consecutive catalytic runs (a, b, c) with intermediate regeneration. $L_{\text{bed}} = 5$ cm, $\text{WHSV} = 4 \text{ h}^{-1}$, $\text{MeOH}:\text{N}_2 = 1:1$, reactor ID 9 mm, set-point 470°C . $\text{C}_{>5}$ indicates hydrocarbons with 5 or more C atoms.

a factor of three in the third run, while product distribution changed towards more short chain olefins, especially C3 and C4 formed at the expense of decreased amounts of paraffins and higher products (Fig. 5b), while Fig. 4 demonstrates that after the first run similar temperature maxima are reached at all three thermocouple positions, suggesting that, already during the first run, the zeolite at the bottom of the bed suffers from steaming. After the third run the catalyst was reg-

enerated and subjected to characterization to explain the observed differences in catalytic behaviour. NH_3 TPD results (Fig. 5c) show a significantly decreased amount of acid sites, while solid-state ^{27}Al NMR indicates formation of extra-framework Al species^{32,33} which are not observed in the parent ZSM-5 (Fig. 5d). These results indicate extensive catalyst dealumination by steaming during the course of reaction, leading to an important loss of acidity and active sites. Weaker acid sites favour olefin formation³⁴ (most likely by partially suppressing the formation of aromatics), while less sites result in a reduced local heat production, both leading to longer catalyst lifetimes, as already demonstrated in literature.³⁵ In turn, higher temperatures result in a larger extent of dealumination and hence even less and weaker acid sites, thus partially explaining a higher olefins (especially propylene) production at higher temperatures (Fig. 1).

Temperature profiles measured when using SiC as diluent (Fig. 3b₁) show much smaller, but not negligible, temperature rises inside the reactor. The product distribution is similar to the one observed for the non-diluted catalyst with slightly lower selectivities to C3–C4 olefins along with longer catalyst lifetimes, in line with the results presented in Fig. 1 and as consequence of the lower overall temperature inside of the reactor. To verify whether radial heat transfer also affects catalyst lifetime, we performed MTH experiments in reactors with different diameter (4, 7, 9 mm) keeping the same bed length and WHSV by adjusting flowrates. No significant differences were found in products selectivity and lifetime when utilizing these reactors (Fig. S3†). These similarities in catalytic performance suggest identical temperature profiles in the radial direction, though one would expect a lower

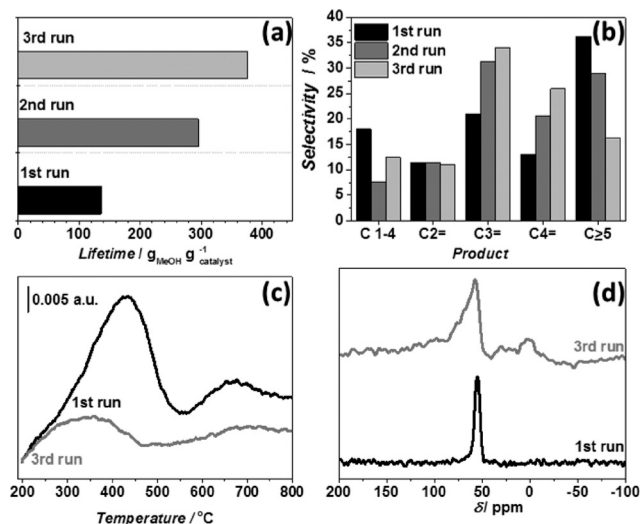


Fig. 5 MTH lifetime over undiluted ZSM-5 in three consecutive runs with regeneration in between tested at 470°C , $L_{\text{bed}} = 5$ cm, $\text{WHSV} = 4 \text{ h}^{-1}$, $\text{MeOH}:\text{N}_2 = 1:1$ (a) and corresponding integral selectivities (b). NH_3 TPD profiles of fresh ZSM-5 and regenerated after three catalytic runs (c) and corresponding ^{27}Al MAS NMR (d).



temperature rise in a reactor with smaller diameter.³⁶ This counterintuitive observation can be explained as a result of interference of a heat effect with acid site effect. In principle, a lower temperature rise in a 4 mm reactor would result in lower extent of dealumination, preserving the stronger acid sites which in turn would lead to a higher coking rate and therefore faster deactivation.

Finally, in view of these findings, we formulated the hypothesis that longer lifetimes generally observed in case of mesoporous ZSM-5 could be -partially- due to the fact that creation of extra pores leads to site isolation and to a lower generation of heat per unit volume of zeolite. In such a case, formation of hot spots should be reduced. Mesoporous ZSM-5 prepared according to the procedure described elsewhere³⁷ was tested in MTH under the same conditions as pristine ZSM-5. Catalytic results (Fig. 3c₁) show a doubled lifetime for the undiluted mesoporous *versus* the pristine ZSM-5, in good agreement with literature.^{7,38–40} The temperature profiles are characterized by three equivalent maxima around 510 °C, thus a $\Delta T = 40$ °C, half of that observed for the parent material. Moreover, significant changes are observed in product distribution. Considerably less paraffins and ethylene while more propylene and butylene are formed (Fig. 3c₂). These results are in clear contrast with the trends observed with the pristine zeolite, where an increase in propylene selectivity was observed upon increasing temperature inside the reactor (*cf.* Fig. 1 and 3). These, *a priori*, controversial results can be explained as a consequence of the desilication process. In spite of the similar Si/Al ratio of the desilicated sample, a lower concentration of acid sites along with a slight decrease in their strength is clear from NH₃-TPD and pyridine adsorption (Fig. S4 and S5[†]). Furthermore, additional pores (empty space) are created, which leads to a decrease in density by 22% for the mesoporous zeolite (Table S2[†]) and to a further reduction in acid site concentration (per zeolite volume). The combination of these two factors leads to the formation of less aromatics³⁴ and to a lower generation of heat per unit catalyst volume, resulting in a higher selectivity to propylene and in prolonged catalyst lifetimes, as experimentally observed. This indicates that not only on the catalyst bed level heat production should be considered, but also on the catalyst particle level. As a consequence, both active site concentration ('site isolation') and their strength should be kept under control to optimize product yield and ZSM-5 catalyst lifetime.

Conclusions

In conclusion, our results demonstrate a strong effect of heat generation inside the catalytic bed on catalyst lifetime in MTH over ZSM-5. The high reaction enthalpy and rate leads to serious difficulties to reach isothermal behaviour during catalyst testing at lab scale, even in the presence of significant amounts of bed diluent. These results partially explain differences found in literature for exactly the same catalytic systems. Moreover, under conditions relevant for industrial application, this specific ZSM-5 zeolite (one of the most

widely reported in literature) can easily undergo extensive *in situ* dealumination by steaming. This fact is often ignored and deserves special attention. Finally, by monitoring temperature inside the catalytic bed for different catalytic systems, we conclude that the prolonged catalyst lifetime of mesoporous ZSM-5 is due to a lower generation of heat per zeolite unit volume and to changes in the acidity of the catalyst upon post-synthetic desilication. Although improvements in diffusion properties after similar procedures have been clearly demonstrated,^{41–44} our results indicate that heat dispersion and catalyst acidity play a more important role in MTH chemistry and associated product selectivity and ZSM-5 catalyst lifetime.

Acknowledgements

This research received funding from the Netherlands Organization for Scientific Research (NWO) in the framework of the TASC Technology Area "Syngas, a Switch to Flexible New Feedstock for the Chemical Industry (TA-Syngas)".

Notes and references

- 1 C. D. Chang and A. J. Silvestri, *J. Catal.*, 1977, **47**, 249–259.
- 2 P. Tian, Y. Wei, M. Ye and Z. Liu, *ACS Catal.*, 2015, **5**, 1922–1938.
- 3 U. Olsbye, S. Svelle, M. Bjorgen, P. Beato, T. V. W. Janssens, F. Joensen, S. Bordiga and K. P. Lillerud, *Angew. Chem., Int. Ed.*, 2012, **51**, 5810–5831.
- 4 J. Gascon, J. R. van Ommen, J. A. Moulijn and F. Kapteijn, *Catal. Sci. Technol.*, 2015, **5**, 807–817.
- 5 J. Perez-Ramirez, C. H. Christensen, K. Egeblad, C. H. Christensen and J. C. Groen, *Chem. Soc. Rev.*, 2008, **37**, 2530–2542.
- 6 S. Lopez-Orozco, A. Inayat, A. Schwab, T. Selvam and W. Schwieger, *Adv. Mater.*, 2011, **23**, 2602–2615.
- 7 M. Bjorgen, F. Joensen, M. S. Holm, U. Olsbye, K.-P. Lillerud and S. Svelle, *Appl. Catal., A*, 2008, **345**, 43–50.
- 8 M. Choi, K. Na, J. Kim, Y. Sakamoto, O. Terasaki and R. Ryoo, *Nature*, 2009, **461**, 246–249.
- 9 M. Milina, S. Mitchell, P. Crivelli, D. Cooke and J. Perez-Ramirez, *Nat. Commun.*, 2014, **5**, 10.
- 10 M. Milina, S. Mitchell, D. Cooke, P. Crivelli and J. Perez-Ramirez, *Angew. Chem., Int. Ed.*, 2015, **54**, 1591–1594.
- 11 N.-L. Michels, S. Mitchell and J. Perez-Ramirez, *ACS Catal.*, 2014, **4**, 2409–2417.
- 12 P. Kumar, J. W. Thybaut, S. Svelle, U. Olsbye and G. B. Marin, *Ind. Eng. Chem. Res.*, 2013, **52**, 1491–1507.
- 13 W. Y. Guo, W. Z. Wu, M. Luo and W. D. Xiao, *Fuel Process. Technol.*, 2013, **108**, 133–138.
- 14 S. Zhang, B. Zhang, Z. Gao and Y. Han, *Ind. Eng. Chem. Res.*, 2010, **49**, 2103–2106.
- 15 D. E. Mears, *J. Catal.*, 1971, **20**, 127–131.
- 16 S. Sartipi, K. Parashar, M. Jose Valero-Romero, V. P. Santos, B. van der Linden, M. Makkee, F. Kapteijn and J. Gascon, *J. Catal.*, 2013, **305**, 179–190.



- 17 C. A. Emeis, *J. Catal.*, 1993, **141**, 347–354.
- 18 I. Yarulina, J. Goetze, C. Gücüyener, L. van Thiel, A. Dikhtiarenko, J. Ruiz-Martinez, B. M. Weckhuysen, J. Gascon and F. Kapteijn, *Catal. Sci. Technol.*, 2016, **6**, 2663–2678.
- 19 W. Wu, W. Guo, W. Xiao and M. Luo, *Fuel Process. Technol.*, 2013, **108**, 19–24.
- 20 W. J. H. Dehertog and G. F. Froment, *Appl. Catal., A*, 1991, **71**, 153–165.
- 21 R. J. Berger, J. Perez-Ramirez, F. Kapteijn and J. A. Moulijn, *Appl. Catal., A*, 2002, **227**, 321–333.
- 22 J. Perez-Ramirez, R. J. Berger, G. Mul, F. Kapteijn and J. A. Moulijn, *Catal. Today*, 2000, **60**, 93–109.
- 23 M. M. Mertens and S. N. Vaughn, ExxonMobil Chemical Patents Inc., 2013.
- 24 D. Mier, A. G. Gayubo, A. T. Aguayo, M. Olazar and J. Bilbao, *AIChE J.*, 2011, **57**, 2841–2853.
- 25 H. Schulz and M. Wei, *Top. Catal.*, 2014, **57**, 683–692.
- 26 H. Schulz, *Catal. Today*, 2010, **154**, 183–194.
- 27 S. Muller, Y. Liu, M. Vishnuvarthan, X. Y. Sun, A. C. van Veen, G. L. Haller, M. Sanchez-Sanchez and J. A. Lercher, *J. Catal.*, 2015, **325**, 48–59.
- 28 S. Ilias and A. Bhan, *J. Catal.*, 2012, **290**, 186–192.
- 29 M. Ibanez, M. Gamero, J. Ruiz-Martinez, B. M. Weckhuysen, A. T. Aguayo, J. Bilbao and P. Castano, *Catal. Sci. Technol.*, 2016, **6**, 296–306.
- 30 D. W. Gardner, J. J. Huo, T. C. Hoff, R. L. Johnson, B. H. Shanks and J. P. Tessonnier, *ACS Catal.*, 2015, **5**, 4418–4422.
- 31 M. Nielsen, R. Y. Brogaard, H. Falsig, P. Beato, O. Swang and S. Svelle, *ACS Catal.*, 2015, **5**, 7131–7139.
- 32 E. Brunner, H. Ernst, D. Freude, T. Frohlich, M. Hunger and H. Pfeifer, *J. Catal.*, 1991, **127**, 34–41.
- 33 C. Ding, X. Wang, X. Guo and S. Zhang, *Catal. Commun.*, 2008, **9**, 487–493.
- 34 M. Westgård Erichsen, K. De Wispelaere, K. Hemelsoet, S. L. C. Moors, T. Deconinck, M. Waroquier, S. Svelle, V. Van Speybroeck and U. Olsbye, *J. Catal.*, 2015, **328**, 186–196.
- 35 M. Stöcker, *Microporous Mesoporous Mater.*, 1999, **29**, 3–48.
- 36 A. Grah, U. Nowak, M. Schreier and R. Adler, *Heat Mass Transfer*, 2009, **45**, 417–425.
- 37 S. Sartipi, M. Alberts, V. P. Santos, M. Nasalevich, J. Gascon and F. Kapteijn, *ChemCatChem*, 2014, **6**, 142–151.
- 38 Y. Wei, P. E. de Jongh, M. L. M. Bonati, D. J. Law, G. J. Sunley and K. P. de Jong, *Appl. Catal., A*, 2015, **504**, 211–219.
- 39 S. L. Zhang, Y. J. Gong, L. L. Zhang, Y. S. Liu, T. Dou, J. Xu and F. Deng, *Fuel Process. Technol.*, 2015, **129**, 130–138.
- 40 J. Kim, M. Choi and R. Ryoo, *J. Catal.*, 2010, **269**, 219–228.
- 41 J. C. Groen, W. Zhu, S. Brouwer, S. J. Huynink, F. Kapteijn, J. A. Moulijn and J. Perez-Ramirez, *J. Am. Chem. Soc.*, 2007, **129**, 355–360.
- 42 J. Perez-Ramirez, C. H. Christensen, K. Egeblad, C. H. Christensen and J. C. Groen, *Chem. Soc. Rev.*, 2008, **37**, 2530–2542.
- 43 J. Karger and R. Valiullin, *Chem. Soc. Rev.*, 2013, **42**, 4172–4197.
- 44 L. Gueudre, M. Milina, S. Mitchell and J. Perez-Ramirez, *Adv. Funct. Mater.*, 2014, **24**, 209–219.

